

## Coherent and Non-Coherent Double Diffractive Production of $Q\bar{Q}$ - pairs in Collisions of Heavy Ions at High Energies.

N.M.Agababyan, S.A.Chatrchyan, A.S.Galoyan, L.L.Jenkovszky <sup>1</sup> A.I.Malakhov,  
G.L.Melkumov, P.I.Zarubin

*Joint Institute for Nuclear Research  
Dubna, Russia*

### Abstract

The double coherent and non-coherent diffractive production of heavy quark - anti-quark pairs ( $Q\bar{Q}$ ) in heavy ion scattering at high energies (LHC) is considered. The total and differential cross sections of these processes with the formation of  $c\bar{c}$  and  $b\bar{b}$  pairs in  $pp$ ,  $CaCa$  and  $PbPb$  collisions are evaluated.

The contribution of the considered mechanisms is a few per cent of the number of heavy quark - antiquark pairs obtained in the processes of hard (QCD) scattering, and it will be taken into account in the registration of  $c$ ,  $b$  quarks or, for instance, in the study of the heavy quarkonia suppression effects in Quark - Gluon Plasma, in the search for intermediate mass Higgs bosons and so on.

It is shown that the cross section of the coherent scattering process is great enough. This makes it suitable for studying collective effects in nuclear interactions at high energies. An example of such effects is given: large values of the invariant mass of a  $Q\bar{Q}$  pair,  $M_{Q\bar{Q}} \gtrsim 100\text{GeV}$ , in association with a large rapidity gap between diffractive jets  $\Delta\eta > 5$ .

---

<sup>1</sup>*Bogolyubov Institute for Theoretical Physics Kiev, Ukraine.*

# Introduction

Over the last decade, interest in studying diffractive processes has increased again. The pronounced features of diffractive (nonperturbative) interactions were observed in the events registered in the experiments carried out at CERN [1], on HERA [2], [3] and Tevatron [4], [5]. First, secondary beams with a large longitudinal momentum ( $x_F \gtrsim 0.9$ ), i.e. with the ejection of a main energy of initial hadrons in a narrow phase space volume (diffraction cone), were registered. Second, an interval in the pseudorapidity space (between these beams), not filled with secondary hadrons ("rapidity gap"), was observed. (As shown, the existence of rapidity gaps (RG) is due to the exchange by a colourless object: a photon,  $W^-$ ,  $Z$  - bosons etc. and, in particular, a Pomeron  $\mathbb{P}$  [6]). Thus, the energy characteristics of the particles involved in the process of scattering were such that these processes fell within the area of QCD applicability. The fraction of such events was:  $\sim 6 \div 7\%$  for  $ep$  interactions [2], [3] and  $\sim 1\%$  for  $p\bar{p}$  interactions [4], [5] of the total number of deep inelastic scattering events. (The theoretical estimates predict a growth of this value for LHC energies up to  $\sim 10 \div 15\%$ , see, for example, [7], [8]). A detailed analysis of the experimental data has shown that they are well described by the assumption of Pomeron exchange.

The hypothesis of Pomerons, first suggested by I.Ya.Pomeranchuk in 1958, was used to explain the behaviour of the total cross section of hadron - hadron interactions within high energies [9]. In the Regge theory, the Pomeron is a colourless object having vacuum quantum numbers. The Regge trajectory corresponds to it:  $\alpha_{\mathbb{P}}(t) = \alpha_{\mathbb{P}}(0) + \alpha' t$ , where  $\alpha_{\mathbb{P}}(0) \simeq 1$ ,  $\alpha' \simeq 0.25 \text{GeV}^{-2}$  and  $t$  is the  $t$ -channel invariant momentum transfer to the Pomeron [10].

In 1985, G. Ingelman and P. Schlein put forward the idea of Pomeron parton structure [11]. It was then verified by the experiments on the research of the diffractive structure function  $F_2^D(\xi, t, z, Q^2)$  [1] - [3].

At the present time, it is supposed that  $F_2^D$  can be presented as a product of the Pomeron structure function  $G_{g/\mathbb{P}}(z, Q^2)$  by the factor of flow  $F_{\mathbb{P}/p}(\xi, t)$  - the hypothesis of factorization <sup>2</sup> [14], [15].

$$F_2^D(\xi, t, z, Q^2) = F_{\mathbb{P}/p}(\xi, t) G_{g/\mathbb{P}}(z, Q^2). \quad (1)$$

The factor of flow describes the number of Pomerons emitted by the hadron. The Pomeron propagator is also included in it. For proton - Pomeron interactions, the following parametrization is most commonly used [14] <sup>3</sup> :

$$F_{\mathbb{P}/p}(\xi, t) = \frac{N_v^2 \beta^2}{4\pi^2} (F_1(t))^2 \xi^{1-2\alpha_{\mathbb{P}}(t)}. \quad (2)$$

---

<sup>2</sup>There is a number of papers, in which the hypothesis of factorization is called in question (see, for example, [12]), but even if factorization is violated for diffractive hard scattering, the effect can be weak at high energies [13]

<sup>3</sup>Other parametrizations of the factor of flow see, for example, in [16]

Here,  $\alpha_{\mathbb{P}}(t)$  is the Pomeron trajectory, the factor  $N_v^2 \beta F_1(t)$  corresponds to the proton - Pomeron interaction vertex;  $\beta = 1.8 \text{ GeV}^{-2}$ ,  $N_v = 3$  is the number of valence quarks in the proton,  $\xi$  is the longitudinal momentum fraction of the Pomeron, and  $F_1(t)$  is the elastic form - factor of the proton, which is parametrized to a high degree of accuracy by the expression:

$$F_1(t) = \frac{4m_p^2 - 2.8t}{4m_p^2 - t} \left(1 - \frac{t}{0.7 \text{ GeV}^2}\right)^{-2}, \quad (3)$$

$m_p$  is the proton mass.

The choice of the Pomeron structure function  $G_{g/\mathbb{P}}(z, Q^2)$  is determined by representing the Pomeron as a composite object. At present, one can mark two conceptually opposite viewpoints of the Pomeron structure<sup>4</sup>. According to one of them, the Pomeron consists of  $q\bar{q}$  - pairs and/or gluons, having small fractions of momentum and slightly different in momentum from one another. It is the so-called "*Soft*" or nonperturbative Pomeron. Its intercept is equal to  $\alpha_{\mathbb{P}}(0) \simeq 1.085$  [8], [14], and the evolution of the structure function is determined by solving the equation of Dokshitzer - Gribov - Lipatov - Altarelli - Parizi (DGLAP) [19]. According to another point of view, the Pomeron is composed of hard gluons and/or  $q\bar{q}$  - pairs. It is the so-called "*Hard*" or perturbative Pomeron. Its intercept equals  $\alpha_{\mathbb{P}}(0) \simeq 1.4$  [20], and the evolution of the structure function is determined by the solution of Balitski - Fadin - Kuraev - Lipatov's equation (BFKL) [21]. The available experimental data [1] - [5] do not allow for the present an unambiguous choice to be made between them. (The mixed "DGLAP - BFKL" representation may be actually realized. However, the integration of both equations requires to introduce a new parameter  $x_0$ , ( $x_0 \simeq 4 \times 10^{-3}$ ), at which the solutions of both equations coincide. The BFKL eq. is solved at  $x < x_0$  and the DGLAP one at  $x \geq x_0$  [22]. According to another very attractive hypothesis, there is a Pomeron with an effective  $Q^2$ - dependence of its intercept, which leads to the observed differences [23]).

Thus, a QCD - motivated study of the formation of various states in diffractive processes at high energies has become possible due to the evolution of the primary Pomeron hypothesis, and the following picture of such mechanisms has arisen:

- i) incident hadron emits a Pomeron (this vertex is described within the framework of the Regge theory and the factor of flow  $F_{\mathbb{P}/p}(\xi, t)$  corresponds to it (2));
- ii) one of the Pomeron partons is involved in hard (QCD) scattering with the production of the investigated state.

For analytical calculations, this means that the structure function of an interacting hadron  $F_2(x, Q^2)$  is substituted by the diffractive structure function  $F_2^D(\xi, t, z, Q^2)$  in the inclusive cross section of the reaction with involved hadrons (1).

The processes of single and double diffraction are distinguished. We are going to follow the definitions from [8], [11], [24] - [26]. Thus, the process of hard Single Diffractive Scattering (*SD*) is the process of hadron scattering, in which one of the primary particles emits a Pomeron, and then it could be in principle registered in the final state (exclusive *SD*) or not (inclusive *SD*). The process of hard Double Diffractive Scattering

---

<sup>4</sup>For the review see, for example, [17], [18] and the literature in them.

( $DD$ ), exclusive and inclusive, is defined in a similar way, and both initial particles emit Pomerons.

The process of uncoupled heavy quark - antiquark pair ( $Q\bar{Q}$ ) production in the proton - proton ( $DD$ ) and Non-Coherent and Coherent ion Double Diffractive scattering ( $NDD$  and  $CDD$ ) at high energies is considered in this paper:

$$p, A + p, A \rightarrow J_D + J_D + Q + \bar{Q} + X, \quad (4)$$

where  $J_D$  depicts a diffractive jet (see Fig. 1). The choice of process (4) is due to a number of reasons:

i) The cross section of this process is larger than the production cross section of rare states ( $W, Z, H$  and so on). This facilitates its registration, especially in the context of studying Double Diffractive scattering and also in the research of collective nuclear effects at high energies;

ii) It is necessary to take into account the contribution of diffractive mechanisms for the registration of  $c$  and  $b$  quarks and also in consideration of other phenomena related to the production or registration of such quarks (for instance, the effect of heavy quarkonia suppression in QGP [27], the search for intermediate mass Higgs bosons [28] and so on).

## Diffractive production of $Q\bar{Q}$ pairs in $pp$ collisions. Basic features.

Let us examine the main points of the calculation of the inclusive double diffractive  $Q\bar{Q}$  production cross section for proton - proton collisions (4) where  $J_D$  is a diffractive jet from the initial proton. The production of a heavy quark pair in single diffractive interactions of protons at high energies has explicitly been studied previously, see, for example, [8], [24] - [30].

As known, the cross section of proton hard scattering (H) can be presented as:

$$\sigma^H(s_0) = \int_{\tau}^1 dx_1 \int_{\tau/x_1}^1 dx_2 \sigma^{part.}(s) [f_{g/p_1}(x_1, Q^2) f_{g/p_2}(x_2, Q^2)], \quad (5)$$

where  $\sigma^{part.}$  is the cross section of reaction (4) at a parton level [31],  $x_1$  and  $x_2$  are the fractions of initial proton momenta carried away by partons involved in the production of a quark pair ( $x_i = q_i/k_i$ ;  $k_i, q_i$  are the 4-momenta of projectiles and quark (antiquark), respectively,  $i = 1, 2$ ),  $\tau = 4m_Q^2/s_0$ , and  $f_{g/p_i}(x_i, Q^2)$  is the distribution function of parton  $g$  in proton  $p_i$ ,  $s_0 = (k_1 + k_2)^2$ ,  $M_{Q\bar{Q}} = (q_1 + q_2)^2$ . Turning to the consideration of diffractive scattering requires to take into account a number of additional points.

Point one. As noted above, according to the hypothesis of factorization, it is necessary to replace both partonic distribution functions  $f_{g/p_i}(x_i, Q^2)$  by diffractive ones (2) in the calculations of  $DD$ , i.e.:

$$f_{g/p_i}(x_i, Q^2) \rightarrow \int_{x_i}^{0.1} \frac{d\xi_i}{\xi_i} \int_{t_{i\min}}^0 dt_i F_{IP_i/p_i}(\xi_i, t_i) G_{g/IP_i}\left(\frac{x_i}{\xi_i}, Q^2\right). \quad (6)$$

Here  $F_{IP_i/p_i}(\xi_i, t_i)$  is the factor of flow (2),  $G_{g/IP_i}(\frac{x_i}{\xi_i}, Q^2)$  is the Pomeron structure function,  $\xi_i = l_i/k_i$ ,  $l_i$  is the Pomeron 4-momentum, and also  $s_{IP} = (l_1 + l_2)^2$ ,  $t_i = (k_i - k_{i_f})^2$ , where  $k_{i_f}$  is the 4-momentum of the incident particle after scattering (diffractive jet  $J_{D_i}$ ). The evolution of the structure functions is calculated at  $Q^2 = M_{Q\bar{Q}}^2$ . The upper limit to the variable  $\xi_i$  is determined by the condition of Pomeron exchange dominance [14], and the lower limit to the variable  $t_i$  is equal to  $t_{i \min} = -s_0(1 - \xi) \frac{\text{Exp}[(-1)^i \eta_i]}{\text{Exp}[\eta_i] + \text{Exp}[-\eta_i]}$  neglecting the proton mass, where  $\eta_i$  is the pseudorapidity of diffractive jet  $J_{D_i}$ ,  $i = 1, 2$ .

As noted above, the choice of the Pomeron structure function  $G_{g/IP}(z, Q^2)$  depends on that which objects, soft or hard, and also a quark and/or a gluon, the Pomeron consists of. As the main mechanism of  $Q\bar{Q}$  production at the parton level is the gluon - gluon one:

$$g + g \rightarrow Q + \bar{Q},$$

gluonic distributions in the Pomeron will be of our interest. With this aim, three parametrizations for the Pomeron gluonic structure function were chosen:

$$zG(z, Q_0^2) = N(1 - z)^5, \quad [11] \quad (7)$$

$$zG(z, Q_0^2) = Nz(1 - z), \quad [13] \quad (8)$$

$$zG(z, Q_0^2) = N(1 - z), \quad [15] \quad (9)$$

most commonly used in the literature <sup>5</sup>. In all cases, the normalization constant  $N$  is determined by the condition:

$$\int_0^1 zG(z, Q_0^2) dz = 1, \quad (10)$$

$Q_0^2 = 4 \text{ GeV}^2$  and  $\Lambda_{QCD} = 0.2 \text{ GeV}$ .

The second point is to take into account the conditions imposed by the requirement of rapidity gap observation.

One can show that the pseudorapidity interval between two diffractive jets  $J_D$  in (4) is equal to [32], [33]:

$$\Delta\eta = \eta_2 - \eta_1 - 2R_{J_D} \simeq \ln \left[ \frac{s_{IP}}{M_{Q\bar{Q}}^2} \right] - 2R_{J_D}. \quad (11)$$

Here,  $R_{J_D}$  is the size of the diffractive jet in the space of azimuthal angle and pseudorapidity (assuming that  $R_{J_D} \simeq 0.7$  [4], [32]. See Fig. 1). In view of the upper limit to the variable  $\xi_{\max} \leq 0.1$ , condition (11) leads to cutting the phase volume accessible for a quark - antiquark pair:

$$M_{Q\bar{Q} \max} \lesssim \frac{\xi_{\max} \sqrt{s_0}}{\text{Exp}(\Delta\eta/2 + R_{J_D})}. \quad (12)$$

Fig. 2 presents the  $M_{Q\bar{Q} \max}$  dependence on  $\Delta\eta$  for different values of  $\sqrt{s_0}$ . As an example, one can see from the figure that the fulfilment of condition (12) results in that the double diffractive production of a pair of  $t$  quarks is prohibited at Tevatron, and their observation

---

<sup>5</sup>Other proposals of the parametrization of the Pomeron structure see, for example, in [13].

in usual  $DD$  at LHC is hardly probable. A similar result was obtained in [25]. At the same time, in collective interactions of ions at LHC, condition (12) can be fulfilled for  $t\bar{t}$ ,  $WW$ ,  $ZZ$  pairs, and such states can be observed [34].

In the above reasonings, it is supposed that the pseudorapidity intervals, corresponding to Pomeron exchange (see. Fig. 1), remain empty. The situation is actually such that these sites turn out to be filled with a certain number of secondary hadrons. This might be due to statistical fluctuations: "leakage through the gap edges" (i.e., there exists a certain probability that hadrons, expected close to the direction of incident particles, occur in the central area fluctuatively) or the result of interaction of other, not "Pomeronic", partons of initial particles - "multiple interaction". These effects are of particular importance when nucleus - nucleus interactions are considered. To take them into account, it was proposed to introduce an additional factor into the expression for diffractive cross section - "survival probability"  $\langle |S|^2 \rangle$  [32] defined as follows. If  $|S(s, b)|^2$  is the probability that two hadrons pass one through another with impact parameter  $b$  at given  $\sqrt{s}$  without interactions, except a hard one, the survival probability can be written as:

$$\langle |S|^2 \rangle = \frac{\int F(b) |S(s, b)|^2 d^2b}{\int F(b) d^2b}, \quad (13)$$

where  $F(b)$  is the usual overlap of partonic densities of interacting hadrons in the space of the impact parameter. The evaluations of  $\langle |S|^2 \rangle$  in various approximations: eikonal, gaussian and some others, give the value of the order of  $\sim 5 \div 23\%$  at LHC energy [32], [35]. With increasing  $\sqrt{s}$ , the value of  $\langle |S|^2 \rangle$  decreases, i.e. it becomes less probable that two hadrons will not interact at high energies (the total cross section  $\sigma_{tot}$  is proportional to the region of soft interaction  $\pi R^2$  in which diffractive scattering happens; this region is in its turn proportional to  $\ln s$ ).

Following the currently accepted estimates,  $\langle |S|^2 \rangle \simeq 10\%$  at  $\sqrt{s} = 14TeV$  for proton - proton interactions.

It should be also emphasized that the filling of rapidity gaps can be due to the so-called "pile up" - effect (the effect of "superposition") when some proton - proton interactions occur in a very small volume. It is obvious that it depends on the intensities of interacting beams. This effect should be kept in mind for LHC. The degree of its influence on experimental results depends on the properties of a registering device. (This problem will be considered in future.)

Fig. 3 presents the calculated results of the differential cross section for quark - antiquark pair production in hard ( $H$ ) and Double Diffractive ( $DD$ ) scatterings of protons:

$$f^{DD,H} = \frac{d^3\sigma^{DD,H}}{dM_{Q\bar{Q}}d\eta_Qd\eta_{\bar{Q}}}, \quad (14)$$

and the ratio

$$R = \frac{d^3\sigma^{DD}}{dM_{Q\bar{Q}}d\eta_Qd\eta_{\bar{Q}}} / \frac{d^3\sigma^H}{dM_{Q\bar{Q}}d\eta_Qd\eta_{\bar{Q}}} 100\%, \quad (15)$$

versus the invariant mass of quark pair  $M_{Q\bar{Q}}$  at  $\eta_Q = \eta_{\bar{Q}} = 0$  and  $\sqrt{s_0} = 14TeV$  for the chosen models of the Pomeron structure function (7) - (9), where  $\eta_{Q,\bar{Q}}$  are the pseudo-rapidities of heavy quarks  $Q, \bar{Q}$ . The solid line corresponds to the evaluation made for hard (QCD) scattering and the dot - dashed, dashed and dotted lines correspond to the evaluations of  $DD$  made using Pomeron models (7), (8) and (9), respectively. The upper limits on  $M_{Q\bar{Q}}$  for different values of rapidity gap  $\Delta\eta$ , calculated from (12), are denoted by straight lines. The factor "survival probability" (13) is not taken into account <sup>6</sup>.

As seen from the figure, the behaviour of the differential cross sections is noticeably different for the considered models of Pomeron. It promotes their recognition in an experiment. The difference in the cross sections is greater than one order of magnitude for the "Soft" (7) and "Hard" (8) models in the region of small invariant masses ( $M_{Q\bar{Q}} \lesssim 50GeV$ ) and it decreases equalizing at  $M_{Q\bar{Q}} \sim 140 \div 180GeV$  for all the models.

As seen from the figure, the production of quark pairs with a large invariant mass and a large gap between diffractive jets (for example,  $M_{Q\bar{Q}} \gtrsim 50GeV$  and  $\Delta\eta > 5$ ) is forbidden. Remind that the maximum allowable value of  $M_{Q\bar{Q}}$  for Double Diffractive  $Q\bar{Q}$  production at  $\sqrt{s_0} = 14TeV$  is approximately  $500GeV$  as it follows from (12).

The fraction of diffractive pairs in the considered kinematical region is an average of  $2 \div 8\%$  of the number of those produced in the hard (QCD) process <sup>7</sup>. This is enough for studying diffractive physics with their aid. At the same time, this fraction is very large and diffractive mechanisms should be taken into account to detect heavy quarks at least in the region of  $M_{Q\bar{Q}} \lesssim 200 \div 500GeV$ .

The total cross sections of heavy quark pair production are obtained by integration (5) over all the variables taking (6) into account. The results are presented in Table 1. It is seen that the fraction of heavy quarks, produced in  $DD$ , is  $\sim 1 \div 18\%$  of the number of those produced in hard scattering. The results obtained in [25] without taking into account the factor  $\langle |S|^2 \rangle$  for  $\sqrt{s_0} = 10TeV$  are presented for comparison. The data obtained by us are a little bit higher than the ones from [25]. This rather well explained by choosing another proton structure function [36].

## Double diffractive production of $Q\bar{Q}$ pairs in collisions of heavy ions.

Let us consider the process of quark - antiquark pair production in the double diffractive scattering of heavy ions. In this case, the calculations are carried out similar to the above described  $DD$  of protons, taking into account that the proton form - factor (3) for coherent scattering is substituted by the nucleus form - factor [26] which we parametrize

---

<sup>6</sup>The factor (13) does not affect the number of produced quark pairs and it must be taken into account when rapidity gaps are only extracted.

<sup>7</sup>It is obvious that this number will be greater for Single Diffraction.

as [37]:

$$F(t) \sim \exp( R_A^2 t / 6 ), \quad (16)$$

where  $R_A$  is the radius of the nucleus  $A$  ( $R_A = r_0 A^{1/3}$ ,  $r_0 = 1.2 fm$ ).

The research of the  $A$  - dependence of the non-coherent diffractive scattering of symmetric nuclei allows the cross section to be parametrized as [37], [38]:

$$\sigma_A \simeq A^{2\alpha} \sigma_N , \quad (17)$$

where the exponent  $\alpha \sim 0.7 \div 0.8$  for peripheral (diffractive) processes [38] and  $\alpha \sim 0.95 \div 1.0$  for central (hard) ones,  $\sigma_N$  is the nucleon - nucleon cross section. We used  $\alpha = 0.7$  for  $NDD$  and  $\alpha = 1.0$  for hard ion scattering.

Fig. 4 presents the dependence of the differential cross section  $f^{NDD,H}$  (14) and ratio  $R(\%)$  (15) on the invariant mass  $M_{Q\bar{Q}}$  for quark - antiquark pair production in the Hard ( $H$ ) and Non-coherent Double Diffractive ( $NDD$ ) scattering of  $Ca$  and  $Pb$  ions for the chosen models of Pomeron (7) - (9). It should be noted that the factor (13) was not taken into account as in case of proton interactions. Note that there are large differences in estimating the value of  $\langle |S|^2 \rangle$  (13) with a variety of approaches. (This problem will be considered in future.) It should be emphasized that the value of  $\langle |S|^2 \rangle$  will be much smaller than for proton - proton collisions in case of  $NDD$  because of multiple collisions of projectile nucleons.

As seen from the figure, the behaviour of the  $NDD$  differential cross section for all models of the Pomeron structure function is similar to the ones in case of proton interactions at  $\sqrt{s_0} = 14 TeV$ . However, the difference between the models is a little bit smaller because of small values of  $\sqrt{s_0}$  ( $\lesssim 10$  at  $M_{Q\bar{Q}} \sim 20 GeV$ ). This leads to that the models become indistinguishable at  $M_{Q\bar{Q}} \sim 50 \div 100 GeV$ . Then, the difference rises rapidly due to that the "Soft" Pomeron (7) is characterized by a sharper fall of the cross section than the "Hard" one (8) with increasing the invariant mass and reaches one order of magnitude at  $M_{Q\bar{Q}} \sim 160 \div 200 GeV$ . As seen from the figure, the production of quark pairs with a large invariant mass and large rapidity gaps (for instance,  $M_{Q\bar{Q}} \gtrsim 30 GeV$  and  $\Delta\eta \geq 5$ ) is forbidden.

Table 2 shows the total cross sections of the hard (central) and non-coherent double diffractive production of heavy quarks and their ratios to the hard one for selected models (7) - (9) in  $CaCa$  and  $PbPb$  interactions. As seen from the table, the fraction of diffractive  $Q\bar{Q}$  pairs averages approximately  $\sim 1(0.01)\%$  of the number of such pairs produced in central  $Ca(Pb)$  collisions.

The coherent double diffractive scattering ( $CDD$ ) was calculated by replacing the proton form - factor (3) by the form - factor of the nucleus [37]. Thus, the total energy of the interacting system is

$$\sqrt{s_A} = A\sqrt{s_0} , \quad (18)$$

neglecting the nucleus mass, where  $\sqrt{s_0}$  is the total energy of nucleon - nucleon interactions ( $\sqrt{s_0} = 5.5 TeV$  for  $PbPb$  beams and  $\sqrt{s_0} = 6.3 TeV$  for  $CaCa$  ones [39]).

Fig. 5 depicts the differential cross section  $f^{CDD}$  (14) versus mass  $M_{Q\bar{Q}}$  in the coherent double diffractive scattering of  $Ca$  and  $Pb$  ions for the selected Pomeron models. In this



case, the factor (13) was not considered in the calculations of the total and differential cross sections. (It should be stressed that the value of  $\langle |S(s, b)|^2 \rangle$  differs from the case of non-coherent scattering here.) As in the previous cases, the upper limits on  $M_{Q\bar{Q}}$  at different  $\Delta\eta$  are denoted by straight lines.

As seen from the figure, in contrast to the previous cases, there is a smoother fall of the cross section with increasing  $M_{Q\bar{Q}}$ . Thus, if the non-coherent cross section of  $Q\bar{Q}$  production at small  $M_{Q\bar{Q}}$  ( $M_{Q\bar{Q}} \lesssim 50\text{GeV}$ ) is larger than the coherent one by one - four orders of magnitude, these cross sections become equal at higher invariant masses ( $M_{Q\bar{Q}} \sim 100 \div 160\text{GeV}$ ), and the coherent cross section becomes larger than the non-coherent one for *Ca* and *Pb* beams at still higher values of  $M_{Q\bar{Q}}$ , for the considered Pomeron models. This difference is stronger for the model of "Soft" Pomeron (7). Such a behaviour follows from a threshold fall of the non-coherent cross section at large  $M_{Q\bar{Q}}$ . Including the total energy of the nucleus (18) in the interaction shifts this threshold to the area of very large invariant masses at given size of a rapidity gap (see Fig. 2). Thus, one can formulate the observation conditions of collective nuclear interactions: the detection of a heavy quark - antiquark pair with a large invariant mass and a large rapidity gap between diffractive jets (for example,  $M_{Q\bar{Q}} > 100\text{GeV}$  at  $\Delta\eta > 3$  or  $M_{Q\bar{Q}} > 50\text{GeV}$  at  $\Delta\eta > 5$  etc.) The coherent cross section is  $\sim 10^{-5} \div 10^{-7}\text{mb}$  in these regions. At the luminosities of heavy ions planned at LHC ( $\sim 10^{26}$  for *PbPb* and  $\sim 10^{30}$  for *CaCa* [40]), this allows one to have up to  $10^4$  such events in a 15- day run ( $10^6\text{s}$ ) of the collider. Medium nuclei ( $A < 100$ ) are more preferable because they have higher luminosities, and so they give larger number of events. Note that the multiplicities of secondary particles are lower in the collisions of light and medium nuclei. It would promote the extraction of a rapidity gap. At the same time, light nuclei do not allow one to move far off the threshold of non-coherent production what complicates the isolation of a pure coherent contribution to the diffractive cross section.

As seen from the figure, the cross sections of coherent scattering differ markedly for the Pomeron models under consideration. Thus, this difference is  $2 \div 3$  orders of magnitude for "Soft" (7) and "Hard" (8) Pomerons and a little bit smaller than one order for the models (7) and (9). Such a behaviour of the cross sections changes weakly in the considered region of invariant masses ( $20\text{GeV} \leq M_{Q\bar{Q}} \leq 200\text{GeV}$ ). As in the previous cases, the cross section of "Hard" Pomerons falls smoother than that for "Soft" ones. However, the region, where the differential cross sections of the studied models coincide, lies far to the higher  $M_{Q\bar{Q}}$  in distinction to proton - proton and non-coherent ion interactions.

The total cross sections of  $c\bar{c}$  and  $b\bar{b}$  pair production in the coherent double diffractive scattering of *CaCa* and *PbPb* are given in Table 3. It should be noted that the total cross section of the "Hard" model (8) is larger for *CaCa* interactions than for *PbPb* ones. The situation is opposite for the models (7) and (9).

## Conclusions.

As it follows from the foregoing, the number of heavy quark pairs produced in double (and, moreover, single) diffractive scattering is a major part of those produced in hard (central) interactions at LHC energies. Therefore, the contribution of diffractive mechanisms should be taken into account as an additional process for the registration of heavy quarks and in the studies of phenomena related to their production or registration (for instance, heavy quarkonia suppression in QGP, search for intermediate mass Higgs boson and so on). At present, the contribution of diffractive mechanisms is small because the values of  $\sqrt{s_0}$  of the running colliders are small. Therefore, a disagreement between theoretical estimates and experimental results is insignificant. It is hoped that the diffractive processes will play an important role in looking for rare states (Higgs particles, new gauge bosons, heavy quarkonia, etc) due to their distinctive features.

On the other hand, the cross sections of diffractive particle production at LHC energies are large enough, and so one can study different aspects of diffractive physics at high energies, namely, the behaviour of structure functions at small  $x$ , the hypothesis of factorization, nuclear shadowing and some other collective nuclear phenomena. Such investigations can be made using the CMS or FELIX setups. They will cover a large interval of pseudorapidity ( $\sim 10$  and  $> 14$  units, respectively) and will have detectors with a high resolution in the central region. Thus, the diffractive cones will be covered and the centrally produced states will be detected, i.e. the complete event could be reconstructed.

The considered invariant mass interval of a centrally produced  $Q\bar{Q}$  pair ( $20\text{GeV} \leq M_{Q\bar{Q}} \leq 200\text{GeV}$ ) is apparently the most optimum one for studying double diffraction at LHC. The cross sections, as well as the masses of produced states, are large enough, which makes for certain event registration. Furthermore, the areas in which the cross sections of the considered models of Pomeron differ significantly for all types of interactions, lie in the mentioned interval of  $M_{Q\bar{Q}}$ .

Finally, note that the study of diffractive interaction is particularly urgent at the first stage of the collider operation, when the beam focusing and luminosity have not reached their designed values yet (i.e., when the fraction of diffractive interactions is larger) and when light and medium nuclei are accelerated.

The authors express their sincere gratitude to M.G.Hayrapetyan and E.A.Strokovsky for fruitful discussions and valuable remarks.

## References

- [1] UA8 Collab., R.Bonio et al., Phys.Lett. **B211**, (1988), 239; UA8 Collab., A.Brandt et al., Phys.Lett. **B297**, (1992), 417.
- [2] H1 Collab., T.Ahmed et al., Phys.Lett. **B348**, (1995), 681; Nucl.Phys. **B429**, (1995), 477; Nucl.Phys. **B439**, (1995), 471.
- [3] ZEUS Collab., M.Derrick et al., Phys.Lett. **B315**, (1993), 481; Phys.Lett. **B332**, (1994), 228; Phys.Lett. **B338**, (1994), 483; Phys.Lett. **B369**, (1996), 55; Z.Phys. **C65**, (1995), 379; Z.Phys. **C68**, (1995), 569.

- [4] CDF Collab., F.Abe et al., Phys.Rev. **D50**, (1994), 5535; Phys.Rev.Lett. **69**, (1992), 3704; Phys.Rev.Lett. **74**, (1995), 855.
- [5] D0 Collab., S.Abachi et al., Phys.Rev.Lett **72**, (1994), 2332; Phys.Rev.Lett **76**, (1996), 734.
- [6] Y.Dokshitzer, V.Khoze, S.Troyan, in Physics in Collision VI, Proc. of the International Conference, Chicago, Illinois, 1986, ed. by M.Derrick, (World Scientific, Singapore, 1987), 365; Yad.Fiz. **46**, (1987), 1220.
- [7] J.D.Bjorken, Int.Jour.Mod.Phys. A **7**, (1992), 4189.
- [8] A.Donnachie, P.Landshoff, Nucl.Phys. **B303**, (1988), 634.
- [9] I.Y.Pomeranchuk, Sov.Phys. JETP **7**, (1958), 499.
- [10] P.D.Collins, An Introduction to Regge Theory and High Energy Physics, Cambridge University Press, (1977).
- [11] G.Ingelman, P.Schlein, Phys.Lett. **B152**, (1985), 256.
- [12] A.Berera, D.E.Soper, "*Behavior of diffractive parton distribution function*", 1996, Preprint Pennsylvania State University, PSU/TH/163;  
A.Berera, "*Jet production cross section with double Pomeron exchange.*", 1997, hep-ph/9705283.
- [13] Z.Kunszt, W.J.Stirling, "*The Parton Interpretation of Hard Diffractive Scattering*", presented at the Workshop on HERA Physics, Durham, 1995; "*Hard Diffractive Scattering: Partons and QCD*", Preprint DTP/96/71; ETH-TH/96-27; hep-ph/9609245.
- [14] A.Donnachie, P.V.Landshoff, Phys.Lett. **B191**, (1987), 309; Phys.Lett. **B198**, (1987), 590; Phys.Lett. **B296**, (1992), 227; Nucl.Phys. **B244**, (1984), 322; Nucl.Phys. **B267**, (1986), 690.
- [15] G.Ingelman K.Janson-Pritz, in Proc. of the "Physics at HERA Workshop", ed. W.Buchmuller and G.Ingelman, Hamburg, 1992, 239; Z.Phys. **C58**, (1993), 285;
- [16] P.Bruni, G.Ingelman, Phys.Lett. **B311**, (1993), 317;  
R.Fiore, L.L.Jenkovszky, F.Paccanoni, Phys.Rev. **D52**, (1995), 6278.
- [17] L.L.Jenkovszky, Ukr.J.Phys. **41**, (1996), 270.
- [18] J.Kwiecinski, in Proc. of "XXVI-th Symposium of Multiparticle Dynamics." Faro, Portugal, 1996; hep-ph/9611306.

- [19] V.N.Gribov, L.N.Lipatov, *Yad.Fiz.* **15**, (1972), 781, 1218; (*Sov.J.Nucl.Phys.*, **15**, (1972), 438, 675);  
 Yu.L.Dokshitzer, *Zh.Eksp.Theor.Phys.* **73**, (1977), 1216; (*Sov.Phys. JETP*, **46**, (1977), 641);  
 G.Altarelli, G.Parisi, *Nucl.Phys.* **B126**, (1977), 298.
- [20] R.Peschanski, S.Wallon, *Phys.Lett.* **B349**, (1995), 357.
- [21] E.A.Kuraev, L.N.Lipatov, V.S.Fadin, *Phys.Lett.* **B60**, (1975), 50;  
 E.A.Kuraev, L.N.Lipatov, V.S.Fadin, *Zh.Eksp.Theor.Phys.* **72**, (1977), 377;  
 (*Sov.Phys. JETP*, **45**, (1977), 199);  
 Ya.Ya.Balitski, L.N.Lipatov, *Yad.Fiz.* **28**, (1978), 1597; (*Sov.J.Nucl.Phys.*, **28**, (1978), 822);  
 L.N.Lipatov, in "Perturbative QCD", ed. by A.H.Mueller, World Scientific, Singapore, 1989, 441;  
 J.B.Bronzan, R.L.Sugar, *Phys.Rev.* **D17**, (1978), 585.
- [22] Ch.Royon, *Ukr.J.Phys.* **41**, (1996), 262.
- [23] A.Capella, A.Kaidalov, C.Merino, J.T.T.Van, *Phys.Lett.*, **B337**, (1994), 358;  
 M.Bertini, M.Giffon, E.Predazzi, *Phys.Lett.* **B349**, (1995), 561;  
 M.Bertini et al., *Rivista Nuovo Cim.*, v. **19**, (1996), 1.
- [24] E.L.Berger, J.C.Collins, D.E.Soper, G.Sterman, *Nucl.Phys.* **B286**, (1987), 704.
- [25] M.Heyssler, "*Diffraction Heavy Flavour Production at the Tevatron and the LHC*", 1996, Preprint DTP/96/10; hep-ph/9602420.
- [26] A.Schafer, O.Nachtmann, R.Schopf, *Phys.Lett.* **B249**, (1990), 331.
- [27] T.Matsui, H.Satz, *Phys.Lett* **B178**, (1986), 416;  
 J.P.Blaizot, Proc. of "Quark Matter" Conference 1988, *Nucl.Phys.* **A498**, (1989), 273.
- [28] Z.Kunszt, S.Moretti, W.J.Stirling, "*Higgs Production at the LHC: an Update on Cross Section and Branching Ratios*" - 1996, Preprint DFTT 34/95; DTP/96/100; Cavendish - HEP - 96/20; ETH-TH -96/48; hep-ph/9611397;  
 M.Heyssler, Z.Kunszt, W.J.Stirling, "*Diffraction Higgs Production at the LHC.*", 1997, Preprint ETH-TH/97-6; DTP/97/08; hep-ph/9702286.
- [29] H.Fritzsch, K.H.Streng, *Phys.lett.* **B164**, (1985), 391;  
 K.H.Streng, *Phys.lett.* **B166**, (1986),443; *Phys.lett.* **B171**, (1986), 313.
- [30] V.Del Duce, "*Theory of Double Hard Diffraction*", 1996, EDINBURGH 96/11; hep-ph/9608454.

- [31] J.F.Owens, Rev.Mod.Phys. **59**, (1987), 465;  
G.Sterman, J.Smith, J.C.Collins et al., Rev.Mod.Phys. **67**, (1995), 157.
- [32] J.D.Bjorken, Phys.Rev. D **47**, (1993), 101.
- [33] J.C.Collins, "*Light-cone Variables, Rapidity and All That*", 1997, hep-ph/9705393.
- [34] S.A.Chatrchyan, P.I.Zarubin, "*Semihard Diffractive Production: the CMS Case*", presented at the "First CMS Heavy Ion Workshop", Lion, France, 1996; 96-122 CMS Document.
- [35] E.Gostman, E.M.Levin, U.Maor, Phys.Lett. **B309**, (1993), 199.
- [36] J.F.Owens, Phys.Lett. **B266**, (1991), 126.
- [37] K.Boreskov, A.Capella, A.Kaidalov, J.Tran Thanh Van, Phys.Rev **D47**, (1993), 919.
- [38] A.Capella, U.Sukhatme, C.-I.Tan, J.Tran Thanh Van, Phys.Rep. **236**, (1994), 225.
- [39] The LHC Study Group, "*The Large Hadron Collider Accelerator Project*", 1993, CERN AC/93-03;  
C.W.Fabjan, "*LHC: Physics, Machine, Experiment*", 1995, CERN - PPE/95-25.
- [40] D.Brandt, K.Eggert, A.Morsch, 1994, CERN AT/94-05 (DI); CERN SL/94-04 (AP); LHC Note 264.

### Table Captions.

Table 1. Total cross sections (mb) of  $c\bar{c}$  and  $b\bar{b}$  pair production in the processes of Hard (QCD) ( $\sigma^H$ ) and Double Diffractive ( $\sigma^{DD}$ ) scattering of protons at different  $\sqrt{s_0}$  using models (7), (8) and (9) of the Pomeron structure function. The gluon distribution in the proton is taken from [36]. The ratio  $R(\%)$  of the total diffractive cross section to the hard one for each model is also given. The results of [25] obtained at  $\sqrt{s_0} = 10TeV$  for model (8) is presented for comparison. The factor (13) is not taken into account.

Table 2. Total cross sections (mb) of  $c\bar{c}$  and  $b\bar{b}$  pair production in the processes of central  $\sigma_A^H$  and Non-Coherent Double Diffractive  $\sigma^{NDD}$  scattering of  $Ca$  and  $Pb$  ions using the Pomeron models (7), (8) and (9). The ratio  $R(\%)$  of the total diffractive cross section to the central one for each model is given too. The factor (13) is not taken into account.

Table 3. Total cross sections  $\sigma^{CDD}$ (mb) of  $c\bar{c}$  and  $b\bar{b}$  pair production in the Coherent Double Diffractive scattering of  $Ca$  and  $Pb$  ions using the above models of Pomeron. The factor (13) is not taken into account.

## Figure Captions.

Figure 1. Schematic representation of heavy quark - antiquark ( $Q\bar{Q}$ ) production in Double Diffractive scattering (4) using the hypothesis of factorization in the plane of azimuthal angle ( $\phi$ ) and pseudorapidity ( $\eta$ ). Projectiles (protons -  $p$  or nuclei -  $A$ ) emit Pomerons ( $\mathbb{P}$ ) and escape producing the diffractive jets ( $J_D$ ), the interval between which ( $\Delta\eta$ ) is a "rapidity gap". The quark - antiquark pair ( $Q\bar{Q}$ ) is produced from the hard (QCD) interaction of both Pomerons. The radius of the diffractive cones in ( $\eta, \phi$ ) is taken equal to  $R_{J_D} \simeq 0.7$ .

Figure 2. Upper (solid lines) and lower (dashed lines) limits on the invariant mass of double diffractively produced heavy quark - antiquark pair  $M_{Q\bar{Q}}(GeV)$  versus rapidity gap size  $\Delta\eta$  for different types of interactions and produced particles: 1 - $PbPb$  Coherent ( $\sqrt{s_0} = 1144TeV$ ), 2 - $CaCa$  Coherent ( $\sqrt{s_0} = 252TeV$ ), 3 - $pp$  ( $\sqrt{s_0} = 14TeV$ ), 4 - $CaCa$  Non-Coherent ( $\sqrt{s_0} = 6.3TeV$  per nucleon), 4 - $PbPb$  Non-Coherent ( $\sqrt{s_0} = 5.5TeV$  per nucleon), t -  $t\bar{t}$  ( $m_t = 175GeV$ ), b -  $b\bar{b}$  ( $m_b = 4.5GeV$ ), c -  $c\bar{c}$  ( $m_c = 1.5GeV$ ).

Figure 3. Dependence of **(a)** the differential cross section of quark - antiquark pair production  $f^{DD,H}(mb/GeV) = \frac{d^3\sigma^{DD,H}}{dM_{Q\bar{Q}}d\eta_Qd\eta_{\bar{Q}}}$  at  $\eta_Q = \eta_{\bar{Q}} = 0$  (14) and **(b)** the ratio  $R(\%) = f^{DD}/f^H$  (15) on the invariant mass of quark pair  $M_{Q\bar{Q}}(GeV)$  for the chosen models of Pomeron: (7) - dot - dashed lines, (8) - dashed lines, (9) - dotted lines, solid line is for hard (QCD) process.  $\sqrt{s_0} = 14TeV$ , the factor (13) is not taken into account. The upper limits on  $M_{Q\bar{Q}}$  for  $\Delta\eta = 3$  and 5 are denoted by vertical lines.

Figure 4. The same as in Fig. 3 only for non-coherent scattering of  $CaCa$  at  $\sqrt{s_0} = 6.3TeV$  per nucleon **(a,c)** and  $PbPb$  at  $\sqrt{s_0} = 5.5TeV$  per nucleon **(b,d)**. The factor (13) is not taken into account.

Figure 5. Dependence of the differential cross section  $f^{CDD}(mb/GeV)$  (14) of  $Q\bar{Q}$  production in the coherent double diffractive scattering of  $CaCa$  **(a)** and  $PbPb$  **(b)** on the invariant mass of pair  $M_{Q\bar{Q}}(GeV)$  at  $\eta_Q = \eta_{\bar{Q}} = 0$  for the chosen models of Pomeron. The designations are the same as in the previous figures. The factor (13) is not taken into account. The upper limits on  $M_{Q\bar{Q}}$  are denoted for  $\Delta\eta = 9,10$  ( $CaCa$ ) and  $\Delta\eta = 12,13$  ( $PbPb$ ) by straight lines.

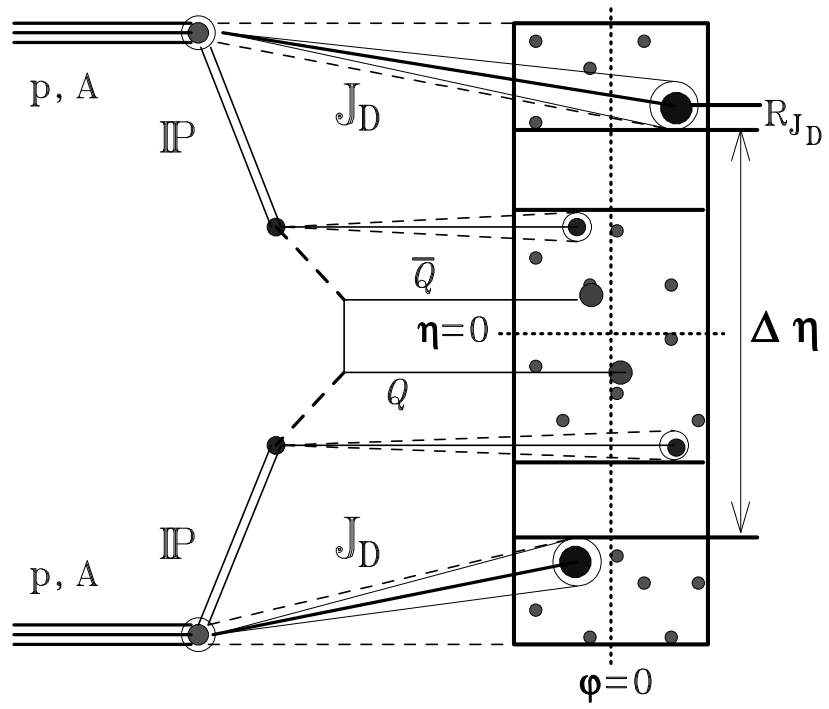


Figure 1:



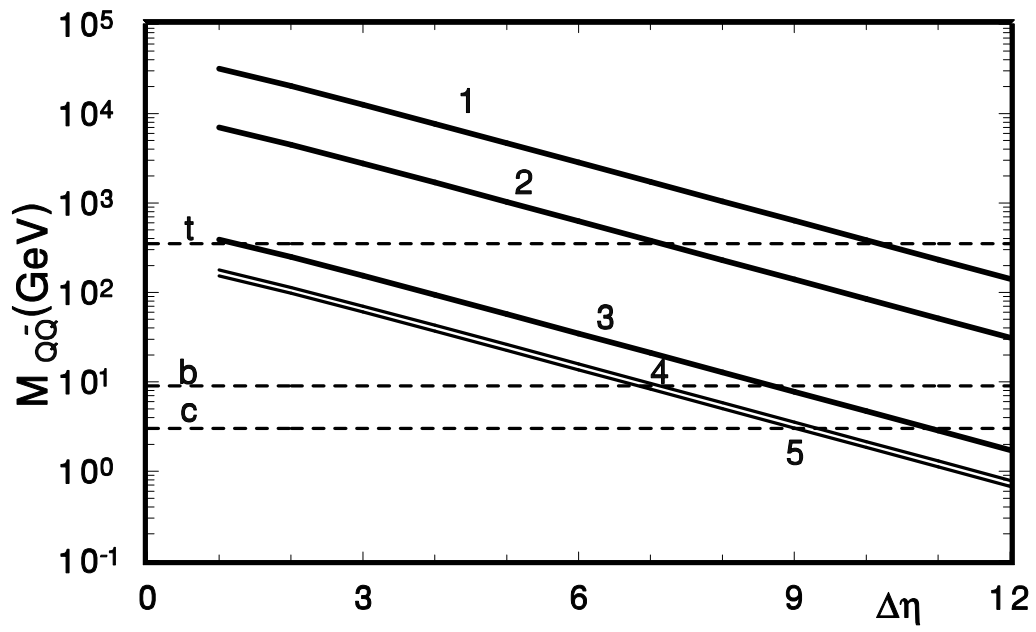


Figure 2:

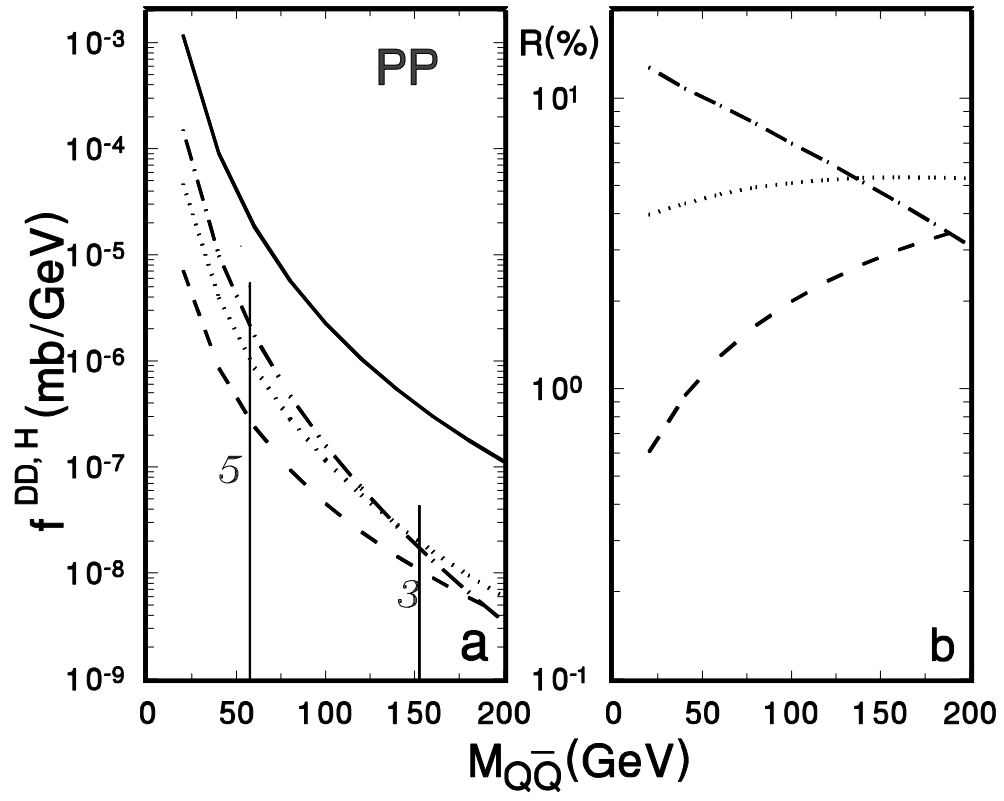


Figure 3:

$\sqrt{s_0} = 14 \text{ TeV}$	$c\bar{c}$	$b\bar{b}$
$\sigma^H$	$1.63 \times 10^{-2}$	$4.49 \times 10^{-3}$
$\sigma^{DD}$ , model (7)	$2.90 \times 10^{-3}$	$2.48 \times 10^{-4}$
$R(\%) = \sigma^{DD}/\sigma^H$	17.79	5.52
$\sigma^{DD}$ , model (9)	$1.40 \times 10^{-3}$	$1.605 \times 10^{-4}$
$R(\%) = \sigma^{DD}/\sigma^H$	8.59	3.575
$\sigma^{DD}$ , model (8)	$1.26 \times 10^{-4}$	$2.76 \times 10^{-5}$
$R(\%) = \sigma^{DD}/\sigma^H$	0.77	0.615
$\sqrt{s_0} = 10 \text{ TeV}$ [25]		
$\sigma^H$	$9.65 \times 10^{-3}$	$2.91 \times 10^{-3}$
$\sigma^{DD}$ , model (8)	$6.56 \times 10^{-5}$	$1.51 \times 10^{-5}$
$R(\%) = \sigma^{DD}/\sigma^H$	0.68	0.52
$\sqrt{s_0} = 6.3 \text{ TeV}$		
$\sigma^H$	$5.12 \times 10^{-3}$	$1.65 \times 10^{-3}$
$\sigma^{DD}$ , model (7)	$3.90 \times 10^{-4}$	$2.75 \times 10^{-5}$
$R(\%) = \sigma^{DD}/\sigma^H$	7.62	1.67
$\sigma^{DD}$ , model (9)	$2.30 \times 10^{-4}$	$2.545 \times 10^{-5}$
$R(\%) = \sigma^{DD}/\sigma^H$	4.49	1.54
$\sigma^{DD}$ , model (8)	$3.27 \times 10^{-5}$	$7.68 \times 10^{-6}$
$R(\%) = \sigma^{DD}/\sigma^H$	0.64	0.465
$\sqrt{s_0} = 5.5 \text{ TeV}$		
$\sigma^H$	$4.27 \times 10^{-3}$	$1.39 \times 10^{-3}$
$\sigma^{DD}$ , model (7)	$2.85 \times 10^{-4}$	$1.90 \times 10^{-5}$
$R(\%) = \sigma^{DD}/\sigma^H$	6.675	1.37
$\sigma^{DD}$ , model (9)	$1.75 \times 10^{-4}$	$1.895 \times 10^{-5}$
$R(\%) = \sigma^{DD}/\sigma^H$	4.10	1.36
$\sigma^{DD}$ , model (8)	$2.71 \times 10^{-5}$	$6.38 \times 10^{-6}$
$R(\%) = \sigma^{DD}/\sigma^H$	0.635	0.46

Table 1:

<i>CaCa</i> , Non-Coherent	$c\bar{c}$	$bb$
$\sigma_A^H$	8.192	2.64
$\sigma^{NDD}$ , model (7)	$6.82 \times 10^{-2}$	$4.81 \times 10^{-3}$
$R(\%) = \sigma^{NDD}/\sigma_A^H$	0.83	0.18
$\sigma^{NDD}$ , model (9)	$4.02 \times 10^{-2}$	$4.45 \times 10^{-3}$
$R(\%) = \sigma^{NDD}/\sigma_A^H$	0.49	0.17
$\sigma^{NDD}$ , model (8)	$5.72 \times 10^{-3}$	$1.34 \times 10^{-3}$
$R(\%) = \sigma^{NDD}/\sigma_A^H$	0.07	0.05
<i>PbPb</i> , Non-Coherent		
$\sigma_A^H$	184.74	60.14
$\sigma^{NDD}$ , model (7)	$5.01 \times 10^{-1}$	$3.34 \times 10^{-2}$
$R(\%) = \sigma^{NDD}/\sigma_A^H$	0.27	0.06
$\sigma^{NDD}$ , model (9)	$3.08 \times 10^{-1}$	$3.33 \times 10^{-2}$
$R(\%) = \sigma^{NDD}/\sigma_A^H$	0.17	0.05
$\sigma^{NDD}$ , model (8)	$4.77 \times 10^{-2}$	$1.12 \times 10^{-2}$
$R(\%) = \sigma^{NDD}/\sigma_A^H$	0.026	0.019

Table 2:

<i>CaCa</i> , Coherent	$c\bar{c}$	$bb$
$\sigma^{CDD}$ , model (7)	$3.58 \times 10^{-2}$	$7.27 \times 10^{-4}$
$\sigma^{CDD}$ , model (9)	$1.14 \times 10^{-2}$	$2.56 \times 10^{-4}$
$\sigma^{CDD}$ , model (8)	$1.01 \times 10^{-4}$	$6.15 \times 10^{-6}$
<i>PbPb</i> , Coherent		
$\sigma^{CDD}$ , model (7)	$6.01 \times 10^{-2}$	$1.43 \times 10^{-3}$
$\sigma^{CDD}$ , model (9)	$1.72 \times 10^{-2}$	$4.43 \times 10^{-4}$
$\sigma^{CDD}$ , model (8)	$1.96 \times 10^{-5}$	$2.46 \times 10^{-6}$

Table 3:

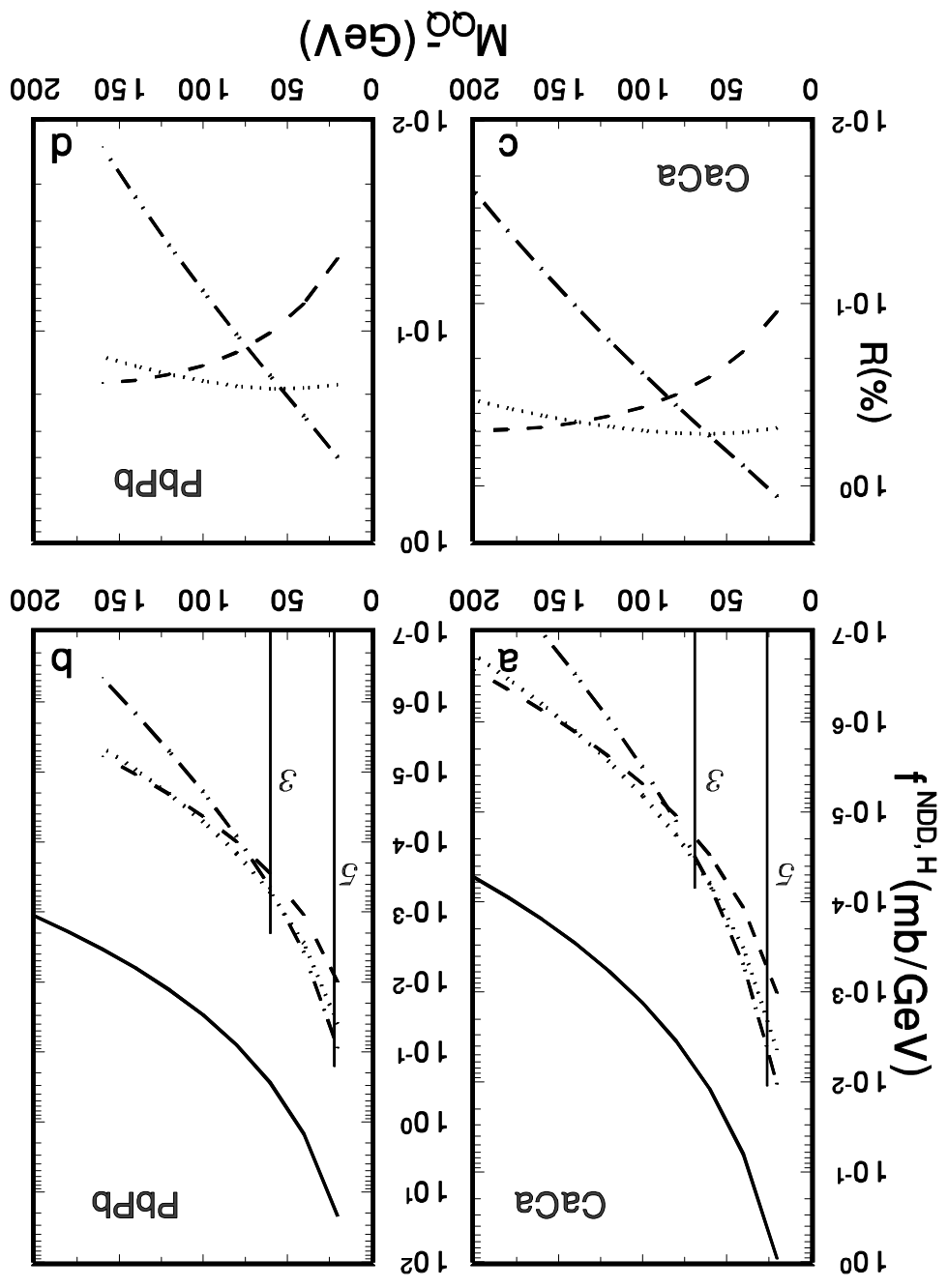


Figure 4:

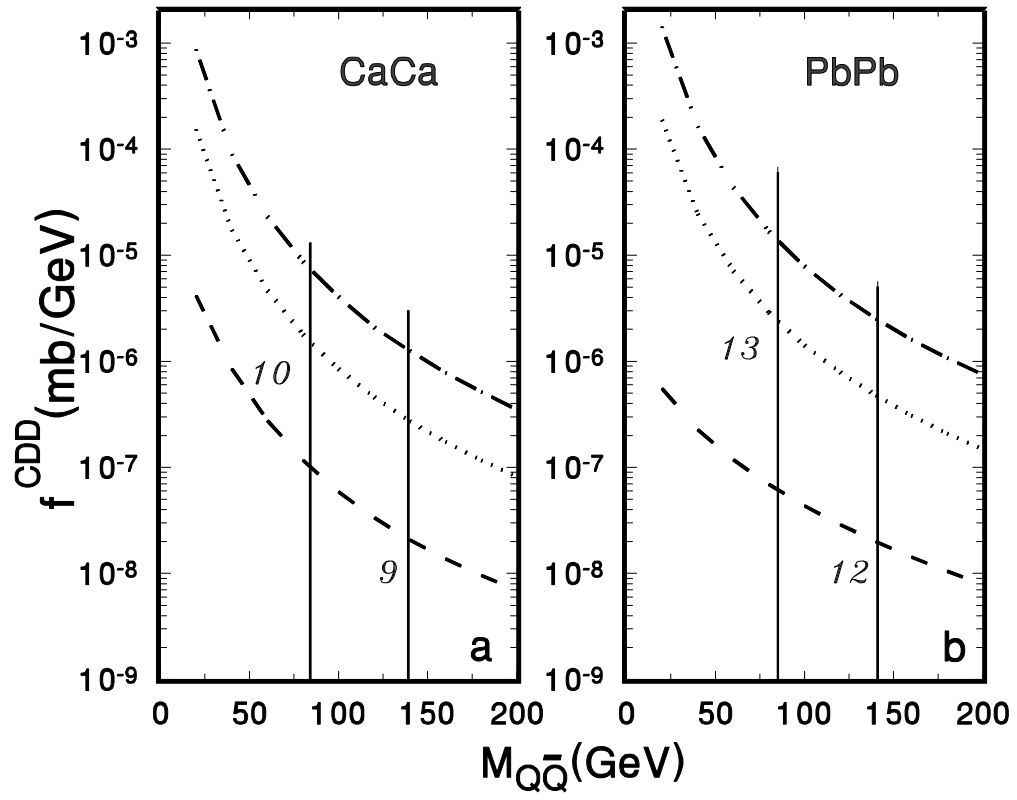


Figure 5: